Proceedings of the 9th International and 49th National Conference on Fluid Mechanics and Fluid Power (FMFP)
December 14-16, 2022, IIT Roorkee, Roorkee-247667, Uttarakhand, India

FMFP2022-XX-YYY

Rotating Waves Arising from the Instability of Magnetized Spherical Couette Flows

Jude Ogbonna[1], Ferran Garcia[2], Thomas Gundrum[1], and Frank Stefani[1]

[1]Institute of Fluid Dynamics, Helmholtz-Zentrum Dresden-Rossendorf, Bautzner Landstr. 400, 01328 Dresden, Germany
[2] Department of Fluid Mechanics, Universitat Politecnica de Catalunya, Av. d'Eduard Maristany, 16, 08019 Barcelona, Spain

ABSTRACT

Rotating waves of various azimuthal wavenumbers appear in magnetized spherical Couette flows in time-dependent states. The criteria for the flow to enter a time-dependent state are determined by the values of Reynolds and Hartmann numbers for a given geometric configuration of the spherical Couette system. These time-dependent states of the flow have been referred to as the radial jet, the return flow and the shear layer instabilities. In the present work, rotating waves in the flow during radial jet and return flow instabilities are observed. The rotating waves both have an azimuthal wavenumber of 3, but vary in their spatial and temporal properties.

Keywords: Experimental fluid dynamics, flow instability, magnetohydrodynamics

I.   INTRODUCTION

The magnetized spherical Couette (MSC) flow occurs when an electrically conducting fluid is utilized in a spherical Couette geometry and a magnetic field is applied to the flow. The resulting flow is governed by the magnetic Prandtl number $Pm = \nu/\eta$ (where ν and η are the kinematic viscosity and the magnetic diffusivity of the fluid, respectively), the Hartmann number $Ha = B_0 r_i/(\mu_0 \rho \nu \eta)^{1/2} = B_0 r_i \sigma^{1/2}/(\rho)^{1/2}$ (where B_0, r_i, μ_0, ρ, and σ are the applied magnetic field, the radius of the inner sphere, the vacuum permeability, the density of the fluid and the electrical conductivity of the fluid, respectively), the ratio of the inner to the outer spheres r_i/r_o (where r_o is the radius of the outer sphere) and the Reynolds number $Re = \Omega r_i^2/\nu$. These parameters sufficiently define the standard magnetized spherical Couette flow, where the inner sphere rotates while the outer sphere remains stationary.

Four different states of the MSC flow have been identified, with one of them being in a steady state while the other three are time-dependent. The steady state of the MSC is its base state, consisting of a flow driven by the rotation of the inner sphere. This rotation flings the fluid outwards by inertia, thus creating a secondary meridional circulation consisting of a narrow jet along the equator towards the outer sphere and a return flow from the rest of the outer sphere towards the origin of the jet[1]. The time-dependent states of the MSC flow are commonly referred to as the radial jet, the return flow and the shear layer instabilities. The physical features of these time-dependent states are described in [1].

The stability curves demarcating the parameter space of Re and Ha into regions representing the base state and the time-dependent states of the MSC flow have been numerically computed for $r_i/r_o = 0.33$[1], 0.5[2], and 0.6[2]. The use of bifurcation lines representing a particular property of the flow is also used to graphically represent the MSC flow states. Various bifurcation diagrams for MSC flows of $r_i/r_o = 0.5$ have been computed[3], [4].

The motivation for the present work is to demonstrate the existence of rotating waves in two different time-dependent states of the MSC flow, namely, the radial jet instability and the return flow instability. The work follows an experimental approach by employing the HEDGEHOG (Hydromagnetic-icExperiment with Differentially Gyrating sphEres HOlding GaInSn) MSC setup at Helmholtz-Zentrum Dresden-Rossendorf.

II.   EQUATIONS

The axial magnetic field $\mathbf{B}_0$ applied to the MSC flow with the spheres rotating about $\hat{\mathbf{e}}_z$, the unit vector representing the z-axis is given in Eq.1

$$\mathbf{B}_0 = B_0 cos(\theta)\hat{\mathbf{e}}_r - B_0 sin(\theta)\hat{\mathbf{e}}_\theta, \tag{1}$$

where B_0, θ, $\hat{\mathbf{e}}_r$, r, and $\hat{\mathbf{e}}_\theta$ are the magnetic field, the colatitude and the unit vectors representing the radial distance and the colatitude, respectively. The Navier-Stokes equation

$$\partial_t \mathbf{v} + \mathbf{v} \cdot \nabla \mathbf{v} = -\nabla p + Re^{-1}\nabla^2 \mathbf{v}$$
$$+ Ha^2 Re^{-1}(\nabla \times \mathbf{b}) \times \hat{\mathbf{e}}_z \tag{2}$$

governs the fluid flow with the no-slip condition applied at the interfaces between the fluid and the spheres. The deviation of the magnetic field induced by the interaction of the flow with B_0 is negligible for Rm ¡¡ 1. This justifies the so-called inductionless approximation of the experiments conducted in the present work since Re = 1000, Pm / 10^{-6} for GaInSn and Rm = RePm. As a result, the induction equation simplifies to

$$0 = \nabla^2 \mathbf{b} + \nabla \times (\mathbf{v} \times \hat{\mathbf{e}}_z). \tag{3}$$

The boundary conditions are assumed to be electrically insulated in accordance with the experiments.

III.   MATERIALS AND METHODS

The setup for the HEDGEHOG, which is the main experimental apparatus, and the geometric relationship between a piezoelectric ultrasonic transducer (a component of the ultrasonic Doppler velocimetry system for measuring the
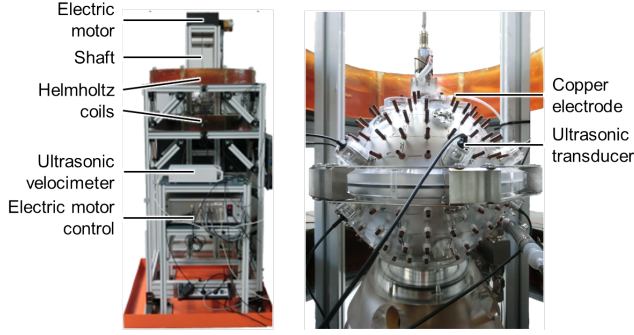
Figure 1: **Photographs of the HEDGEHOG setup showing its full view (left) and a close-up view on the outer sphere (right).**

fluid velocities) and the HEDGEHOG spheres are shown in Fig. 1.

A. Experimental apparatus and instrumentation

The inner and outer spheres of HEDGEHOG are made from acrylic glass. Their radii are 45 mm and 90 mm, respectively. Thus, r i /r o is fixed at 0.5. The inner sphere is rotated by an electric motor shaft passing through the poles of both spheres. The diameter of the shaft between the inner and outer spheres is only 3 mm, so that the interference caused by its rotation on the major fluid flow is insignificant. GaInSn completely fills the volume between the inner and outer spheres. GaInSn is a eutectic alloy of gallium (67 % by mass), indium (20.5 % by mass) and tin (12.5 % by mass). A lead weight inside the inner sphere counterbalances the buoyancy force exerted by the density of GaInSn. The outer surface of the outer sphere contains provisions for mounting the ultrasonic transducers. The surface also contains 168 needle-like copper electrodes for electric potential measurement, rendering it with the distinctive appearance that inspired its name. The axial magnetic field for the flow is generated by current through a Helmholtz coil pair of 80 wire windings in each coil. The radius of each coil and the distance between them are both approximately 300 mm.

The associated instrumentation for the HEDGEHOG experimental setup is the ultrasonic Doppler velocimetry system, consisting of piezoelectric ultrasonic transducers (Signal Processing SA, model TR0410LS) and an ultrasonic Doppler velocimeter (Signal Processing SA, model DOP3010). For the present experiments, six transducers were used at colatitudes of 78.9° with respect to the spheres. Each transducer was inclined southward so that the angle between the axis of the transducer and the equator of the spheres was 35°. Each transducer periodically emitted an ultrasonic pulse at a frequency of 4 MHz and received the echoes from the particles in the path of the ultrasonic beam. These particles are formed as a result of the oxidation of GaInSn due to its exposure to air. From each transducer channel, the velocimeter sequentially acquired the echo signals reflected by the particles to determine the velocities of the flow parallel to each transducer axis.
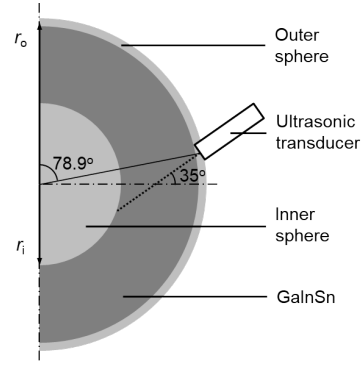

Figure 2: **Meridional section showing the geometric relations for one of the six azimuthally equidistant ultrasonic transducers installed on HEDGEHOG. The dotted line extending from the ultrasonic transducer represents its line of view along which the flow velocity components parallel to the line were measured.**

Table 1: **Physical properties of GaInSn[5]**

ρ (kg m^{-3})	ν (m^2 s^{-1})	$\eta = 1/\mu_0\, \sigma$ (m^2 s^{-1})
6.4×10^3	3.4×10^{-7}	0.2428

B. Procedure

Since ultrasonic Doppler velocimetry relies on the reflection of the ultrasonic pulses by the naturally-occurring oxides in GaInSn, the oxides were distributed by circulating the GaInSn from the north pole to the south pole via a peristaltic pump connected to the poles externally. The axial magnetic field B 0 was calculated from the current I through the Helmholtz coil pair from the relation

$$\mathbf{B}_0 = \frac{(4/5)^{3/2}\mu_0 nI}{R}, \tag{4}$$

where n and R are the number of wire windings in each Helmholtz coil and the radius of each coil (which is equal to the distance between the coils), respectively.

Two sets of experiments were conducted, one at Ha = 5 and and the other at Ha = 35. Both sets of experiments were conducted at Re = 1000. At Re = 1000 and Ha = 5, the flow is in the state of radial jet instability, while the flow is in the state of return flow instability at Re = 1000 and Ha = 35. Thus, the MSC flows at two distinct time-dependent states were investigated. The values of Re and Ha were evaluated using the properties of GaInSn given in Table 1.

The results of the experiments were inferred from the velocity data measured by ultrasonic Doppler velocimetry. The velocity data were sampled at approximately 1.17 seconds per data point. This difference in the measured time between the six transducers were ignored since they are negligible compared to the period of the rotating waves generated in the flow. One hour of the velocity data was analysed for each experiment.
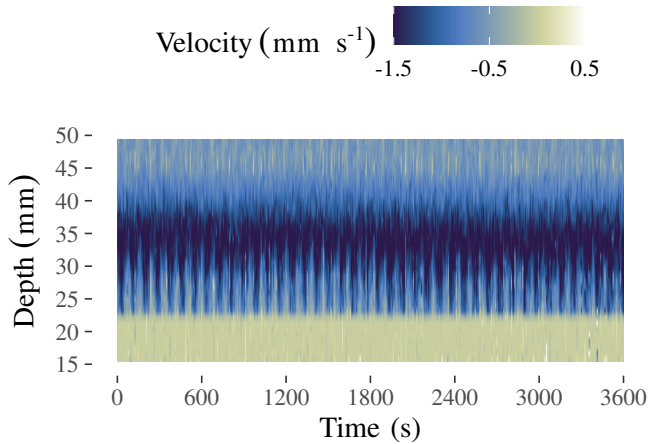
Figure 3: **Plots of the experimentally measured velocity components parallel to the ultrasonic transducer axis at Ha = 5 and Re = 1000. The depth indicates the axial distance from the ultrasonic transducer.**
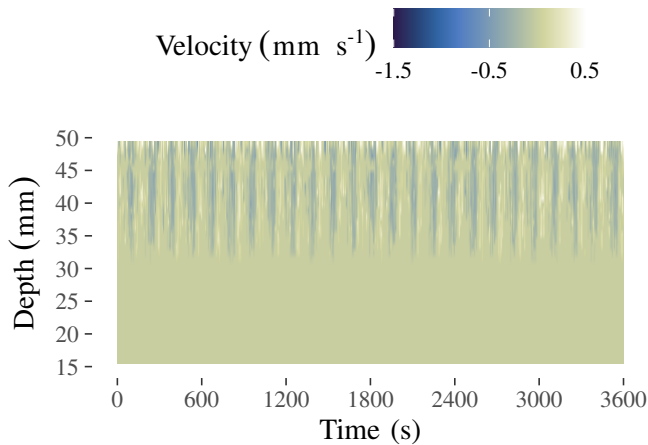

Figure 4: **Plots of the experimentally measured velocity components parallel to the ultrasonic transducer axis at Ha = 35 and Re = 1000. The depth indicates the axial distance from the ultrasonic transducer.**

IV. RESULTS
A. Flow velocities

Figures 3 and 4 show the plots of the velocity components of the flow along the axis of one of the six ultrasonic transducers for Ha = 5 and 35, respectively. The depths indicate the distance away from the transducer along its axis. The sign convention of the velocity is such that flows away from the transducers have positive velocities, while flows towards the transducers have negative velocities.
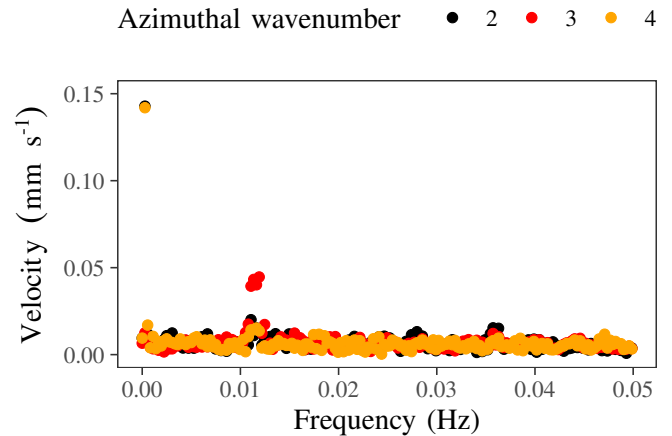

Figure 5: **Velocities of the flow decomposed into azimuthal wavenumbers 2, 3 and 4 obtained from the discrete Fourier transform of the velocity data at Ha = 5 and Re = 1000.**

B. Azimuthal modes

The base and time-dependent states of the MSC flow differ by the absence of kinetic energy in the non-axisymmetric azimuthal modes in the former. The kinetic energy correlates with the velocity of the azimuthal modes. The velocities in the azimuthal modes are obtained from the two-dimensional fast Fourier transform (FFT) of the velocity data in time and space (using the velocity data captured by each of the six ultrasonic transducers). The azimuthal modes of the MSC flow correspond to the azimuthal wavenumbers of the rotating waves present in the flow.

Figures 5 and 6 show the velocities of the various azimuthal modes in the flow for Ha = 5 and 35, respectively. The dominant azimuthal modes correspond to the azimuthal wavenumber m of the rotating wave in the flow. The FFT for Ha = 5 and 35 were taken at depths of approximately 30 mm and 40 mm, respectively (refer to Figs. 3 and 4 for the depths). The results show that $m = 3$ for rotating waves in both flows. However, the frequency of the rotating wave at Ha = 5 is approximately 0.012 Hz, whereas it is approximately 0.007 Hz for Ha = 35. Furthermore, the rotating waves in the two flows are dominant at different depths. This can be inferred from the structure of the velocity plots in Figs. 3 and 4, and determined the depths at which the FFT of the velocity data were conducted.

V. CONCLUSIONS

Experiments were conducted at two time-dependent states of the MSC flow at Ha = 5 for the radial jet instability and at Ha = 35 for the return flow instability, both at Re = 1000. In both cases, rotating waves of $m = 3$ were observed. However, the rotating waves in the two flows differed in their frequencies and the depths at which they were dominant, owing to the differences in the spatial structures of the flow in the radial jet and the return flow
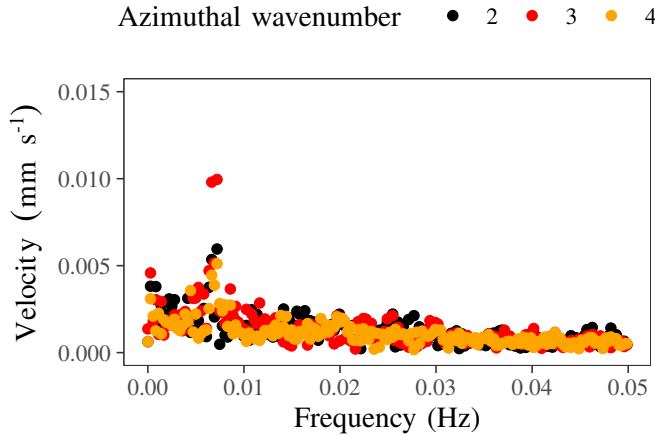
3

Figure 6: **Velocities of the flow decomposed into azimuthal wavenumbers 2, 3 and 4 obtained from the discrete Fourier transform of the velocity data at Ha = 35 and Re = 1000.**

instabilities.

REFERENCES

[1] R. Hollerbach, "Non-axisymmetric instabilities in magnetic spherical Couette flow," *Proc. R. Soc. A*, vol. 465, no. 2107, pp. 2003–2013, 2009.

[2] V. Travnikov, K. Eckert, and S. Odenbach, "Influence of an axial magnetic field on the stability of spherical Couette flows with different gap widths," *Acta Mech.*, vol. 219, pp. 255–268, Jul 2011.

[3] F. Garcia and F. Stefani, "Continuation and stability of rotating waves in the magnetized spherical Couette system: secondary transitions and multistability," *Proc. R. Soc. A*, vol. 474, no. 2220, p. 20180281, 2018.

[4] F. Garcia, M. Seilmayer, A. Giesecke, and F. Stefani, "Modulated rotating waves in the magnetized spherical Couette system," *J. Nonlinear Sci.*, vol. 29, pp. 2735–2759, 2019.

[5] G. Rüdiger, L. L. Kitchatinov, and R. Hollerbach, *Magnetic processes in astrophysics : theory, simulations, experiments*. 2013.